ICES REPORT 15-11

April 2015

Integration over curves and surfaces defined by the closest point mapping

by

C. Kublik and R. Tsai

The Institute for Computational Engineering and Sciences
The University of Texas at Austin
Austin, Texas 78712

Reference: C. Kublik and R. Tsai, "Integration over curves and surfaces defined by the closest point mapping," ICES REPORT 15-11, The Institute for Computational Engineering and Sciences, The University of Texas at Austin, April 2015.

Integration over curves and surfaces defined by the closest point mapping

Catherine Kublik* and Richard Tsai†

Abstract

We propose a new formulation using the closest point mapping for integrating over smooth curves and surfaces with boundaries that are described by their closest point mappings. Contrary to the common practice with level set methods, the *volume integrals* derived from our formulation coincide exactly with the surface or line integrals that one wish to compute. We study various aspects of this formulation and provide a geometric interpretation of this formulation in terms of the singular values of the Jacobian matrix of the closest point mapping. Additionally, we extend the formulation - initially derived to integrate over manifolds of codimension one - to include integration along curves in three dimensions. Some numerical examples are presented.

1 Introduction

This paper provides simple formulations for integrating over manifolds of codimensions one, or two in $\mathbb{R}^3$, when the manifolds are described by functions that map points in $\mathbb{R}^n$ $(n = 2, 3)$ to their closest points on curves or surfaces using the Euclidean distance. The idea for the formulation originated in [7] where the authors proposed a formulation for computing integrals of the form

$$\int_{\partial\Omega} v(\mathbf{x}(s))ds, \tag{1}$$

in the level set framework, namely when the domain Ω is represented implicitly by the signed distance function to its boundary $\partial\Omega$. Typically in a level set method [11, 12, 14], to evaluate an integral of the form of (1) where $\partial\Omega$ is the zero level set of a continuous function φ, it is necessary to extend the function v defined on the

*Department of Mathematics, University of Dayton, Dayton, OH 45469.

†Department of Mathematics and Institute for Computational Engineering and Sciences, University of Texas at Austin, Austin, TX 78712, and KTH Royal Institute of Technology, Stockholm, Sweden.

boundary $\partial\Omega$ to a neighborhood in $\mathbb{R}^n$. The extension of v, denoted $\tilde{v}$, is typically a constant extension of v. The integral is then *approximated* by an integral involving a regularized Dirac-δ function concentrated on $\partial\Omega$, namely

$$\int_{\partial\Omega} v(\mathbf{x}(s))ds \approx \int_{\mathbb{R}^n} \tilde{v}(\mathbf{x})\delta_\epsilon(\varphi(\mathbf{x}))|\nabla\varphi(\mathbf{x})|d\mathbf{x}.$$

Various numerical approximations of this delta function have been proposed, see e.g. [3, 2, 15, 16, 17].

In [7], with the choice of $\varphi = d_{\partial\Omega}$ being a signed distance function to $\partial\Omega$, the integral (1) is expressed as an average of integrals over nearby level sets of $d_{\partial\Omega}$, where these nearby level sets continuously sweep a thin tubular neighborhood around the boundary $\partial\Omega$ of radius ϵ. Consequently, (1) is *equivalent* to the volume integral shown on the right hand side below:

$$\int_{\partial\Omega} v(\mathbf{x}(s))ds = \int_{\mathbb{R}^n} v(\mathbf{x}^*)J(\mathbf{x}; d_{\partial\Omega})\delta_\epsilon(d_{\partial\Omega}(\mathbf{x}))d\mathbf{x}, \tag{2}$$

where δ_ϵ is an averaging kernel, $\mathbf{x}^*$ is the closest point on $\partial\Omega$ to $\mathbf{x}$ and $J(\mathbf{x}; d_{\partial\Omega})$ accounts for the change in curvature between the nearby level sets and the zero level set.

Now suppose that $\partial\Omega$ is a smooth hypersurface in $\mathbb{R}^3$ and assume that $\mathbf{x}$ is sufficiently close to Ω so that the closest point mapping

$$\mathbf{x}^* = P_{\partial\Omega}(\mathbf{x}) = \text{argmin}_{y\in\partial\Omega}|\mathbf{x} - \mathbf{y}|$$

is continuously differentiable. Then the restriction of $P_{\partial\Omega}$ to $\partial\Omega_\eta$ is a diffeormorphism between $\partial\Omega_\eta$ and $\partial\Omega$, where $\partial\Omega_\eta := \{\mathbf{x} : d_{\partial\Omega}(\mathbf{x}) = \eta\}$. As a result, it is possible to write integrals over $\partial\Omega$ using points on $\partial\Omega_\eta$ as:

$$\int_{\partial\Omega} v(\mathbf{x})dS = \int_{\partial\Omega_\eta} v(\mathbf{x}^*)J(\mathbf{x}; \eta)dS,$$

where $J(\mathbf{x}, \eta)$ comes from the change of variable defined by $P_{\partial\Omega}$ restricted on $\partial\Omega_\eta$. Averaging the above integrals respectively with a kernel, δ_ϵ, compactly supported in $[-\epsilon, \epsilon]$, we obtain

$$\int_{\partial\Omega} v(\mathbf{x})dS = \int_{-\epsilon}^{\epsilon} \delta_\epsilon(\eta) \int_{\partial\Omega_\eta} v(\mathbf{x}^*)J(\mathbf{x}; \eta)dS\ d\eta.$$

Formula (2) then follows from the coarea formula [5] applied to the integral on the right hand side.

This paper is motivated by the recent success in the closest point methods for solving partial differential equations on surfaces [8, 9, 10, 13] as well as the need to process data sets that contain unstructured points sampled from some underlying

surfaces. In the following section, we show that in three dimensions the Jacobian J in (2) is the product of the first two singular values, σ_1 and σ_2, of the Jacobian matrix of the closest point mapping $\frac{\partial P_{\partial\Omega}}{\partial \mathbf{x}}$; namely,

$$\int_{\partial\Omega} v(\mathbf{x}(s))ds = \int_{\mathbb{R}^3} v(P_{\partial\Omega}(\mathbf{x}))\delta_\epsilon(d_{\partial\Omega}(\mathbf{x}))\prod_{j=1}^{2}\sigma_j(\mathbf{x})d\mathbf{x}.$$

To motivate the new approach using singular values, we consider Cartesian coordinate systems with the origin placed on points sufficiently close to the surface, and the z direction normal to the surface. Thus the partial derivatives of the closest point mapping in the z direction will yield zero and the partial derivative in the other two directions naturally correspond to differentiation in the tangential directions. Thus we see that one of the singular values should be 0 while the other two are related to the surface area element. We also derive a similar formula for integration along curves in three dimensions (codimension 2). The advantages of this new formula include the ease for constructing higher order approximations of J via e.g. simple differencing, even in neighborhoods of surface boundaries where curvatures become unbounded.

For clarity of the exposition in the rest of the paper, we will now denote the distance function simply by d.

2 Integration using the closest point mapping

In this section, we relate the Jacobian J in (2) to the singular values of the Jacobian matrix of the closest point mapping from $\mathbb{R}^2$ or $\mathbb{R}^3$ to Γ, where Γ denotes the curves or surfaces on which integrals are defined. We assume that in three dimensions, if Γ is not closed, it has smooth boundaries.

2.1 Codimension 1

We consider a C^2 compact curve or surface Γ that can either be closed or not. If Γ is closed, then it is the boundary of a domain Ω so that Γ can be denoted $\partial\Omega$. If Γ is not closed, we assume that it has smooth boundaries. We define $d : \mathbb{R}^n \mapsto \mathbb{R} \cup \{0\}$ to be the distance function to Γ and P_Γ to be the closest point mapping $P_\Gamma : \mathbb{R}^n \mapsto \Gamma$ (for $n = 2, 3$) defined as

$$|P_\Gamma(\mathbf{x}) - \mathbf{x}| = \min_{\mathbf{y}\in\Gamma} |\mathbf{y} - \mathbf{x}|. \tag{3}$$

We let d_0 be the distance function to Γ if it is open and d_s be the signed distance function to $\Gamma = \partial\Omega$ if it is closed. The signed distance function is defined as

$$d_s(\mathbf{x}) := \begin{cases} \inf_{\mathbf{y}\in\Omega^c} |\mathbf{x} - \mathbf{y}| & \text{if } \mathbf{x} \in \Omega, \\ -\inf_{\mathbf{y}\in\Omega} |\mathbf{x} - \mathbf{y}| & \text{if } \mathbf{x} \in \bar{\Omega}^c. \end{cases}$$

Then we define d as follows:

$$d(\mathbf{x}) := \begin{cases} d_0(\mathbf{x}) & \text{if } \Gamma \text{ is open,} \\ d_s(\mathbf{x}) & \text{if } \Gamma \text{ is closed.} \end{cases} \tag{4}$$

Lemma 1. *Let d be the distance function to Γ defined in (4). For $|\eta|$ sufficiently close to 0, the Gaussian curvature at a point on the η level set $\Gamma_\eta := \{\xi : d(\xi) = \eta\}$ can be expressed as*

$$G_\eta = d_{xx}d_{yy} + d_{xx}d_{zz} + d_{yy}d_{zz} - d_{xy}^2 - d_{xz}^2 - d_{yz}^2. \tag{5}$$

Proof. Starting with the definition of the Gaussian curvature G for a surface (see [6]), we can obtain an expression for the Gaussian curvature of its η-level set in terms of d as

$$\begin{aligned} G &= \langle \nabla d, adj(Hess(d))\nabla d \rangle \\ &= d_x^2(d_{yy}d_{zz} - d_{yz}^2) + d_y^2(d_{xx}d_{zz} - d_{xz}^2) + d_z^2(d_{xx}d_{yy} - d_{xy}^2) \\ &\quad + 2[d_x d_y(d_{xz}d_{yz} - d_{xy}d_{zz}) + d_y d_z(d_{xy}d_{xz} - d_{yz}d_{xx}) \\ &\quad + d_x d_z(d_{xy}d_{yz} - d_{xz}d_{yy})]. \end{aligned} \tag{6}$$

We show that this expression is the same as (5) by rearranging the terms above and using the fact that close to Γ the distance function satisfies $|\nabla d| = 1$. First we rearrange the terms in G:

$$\begin{aligned} G \;=\; & d_x^2 d_{yy}d_{zz} + d_y^2 d_{xx}d_{zz} + d_z^2 d_{xx}d_{yy} - d_x^2 d_{yz}^2 - d_y^2 d_{xz}^2 - d_z^2 d_{xy}^2 \\ & + 2[d_x d_y(d_{xz}d_{yz} - d_{xy}d_{zz}) + d_y d_z(d_{xy}d_{xz} - d_{yz}d_{xx}) + d_x d_z(d_{xy}d_{yz} - d_{xz}d_{yy})], \end{aligned}$$

and rewrite each of the first six terms in terms of $|\nabla d|^2$, e.g.

$$d_x^2 d_{yy}d_{zz} = \underbrace{|\nabla d|^2}_{=1} d_{yy}d_{zz} - d_y^2 d_{yy}d_{zz} - d_z^2 d_{yy}d_{zz} = d_{yy}d_{zz} - d_y^2 d_{yy}d_{zz} - d_z^2 d_{yy}d_{zz}.$$

Thus we have

$$\begin{aligned} & d_x^2 d_{yy}d_{zz} + d_y^2 d_{xx}d_{zz} + d_z^2 d_{xx}d_{yy} - d_x^2 d_{yz}^2 - d_y^2 d_{xz}^2 - d_z^2 d_{xy}^2 \\ = \; & \underbrace{d_{xx}d_{yy} + d_{xx}d_{zz} + d_{yy}d_{zz} - d_{xy}^2 - d_{xz}^2 - d_{yz}^2}_{=G_\eta} - d_y^2 d_{yy}d_{zz} - d_z^2 d_{yy}d_{zz} \\ & - d_x^2 d_{xx}d_{zz} - d_z^2 d_{xx}d_{zz} - d_y^2 d_{xx}d_{yy} - d_x^2 d_{xx}d_{yy} \\ & + d_y^2 d_{yz}^2 + d_z^2 d_{yz}^2 + d_x^2 d_{xz}^2 + d_z^2 d_{xz}^2 + d_x^2 d_{xy}^2 + d_y^2 d_{xy}^2 \end{aligned} \tag{7}$$

Using (7) and rearranging the rest of the terms in (6) we obtain $G = G_\eta$. □

Proposition 2. *Consider a C^2 compact surface $\Gamma \subset \mathbb{R}^n$ ($n = 2, 3$) of codimension 1 and let d be defined as in (4). Define the closest point projection map P_Γ as in (3) for $\mathbf{x} \in \mathbb{R}^n$. For $|\eta|$ sufficiently close to zero, let Γ_η be the η level set of d*

$$\Gamma_\eta := \{\mathbf{x} : d(\mathbf{x}) = \eta\}. \tag{8}$$

Define the Jacobian J_η as

$$J_\eta := \begin{cases} 1 + \eta\kappa_\eta & \text{if } n = 2, \\ 1+2\eta H_\eta + \eta^2 G_\eta & \text{if } n = 3, \end{cases}$$

where κ_η is the signed curvature of Γ_η in 2D, and H_η and G_η are its Mean curvature and Gaussian curvature respectively in 3D.

Then if $\frac{\partial P_\Gamma}{\partial \mathbf{x}}$ is the Jacobian matrix of P_Γ we have

$$J_\eta = \begin{cases} \sigma_1, & n = 2, \\ \sigma_1\sigma_2, & n = 3, \end{cases} \tag{9}$$

where σ_1, σ_2 are the first two singular values of the Jacobian matrix $\frac{\partial P_\Gamma}{\partial \mathbf{x}}$.

Proof. The distance function d satisfies the property $d(\mathbf{x}) = 0$ for $\mathbf{x} \in \Gamma$. Also, since Γ is C^2, its distance function d belongs to $C^2(\mathbb{R}^n, \mathbb{R})$; see e.g. [1, 4]. It follows that the order of the mixed partial derivatives does not matter. In addition, the normals to a smooth interface do not focus right away so that the distance function is smooth in a tubular neighborhood T around Γ, and is linear with slope one along the normals. Therefore we have

$$|\nabla d| = 1 \text{ for all } \mathbf{x} \in T. \tag{10}$$

The third important fact is that the Laplacian of d at a point $\mathbf{x}$ gives (up to a constant related to the dimension) the mean curvature of the isosurface of d passing through $\mathbf{x}$, namely

$$\Delta d(\mathbf{x}) = (1 - n)H(\mathbf{x}), \tag{11}$$

where $H(\mathbf{x})$ is the Mean curvature of the level set $\{\mathbf{y} : d(\mathbf{y}) = d(\mathbf{x})\}$. Differentiating (10) with respect to each variable gives the following equations in three dimensions:

$$d_x d_{xx} + d_y d_{xy} + d_z d_{xz} = 0, \tag{12}$$
$$d_x d_{yx} + d_y d_{yy} + d_z d_{yz} = 0, \tag{13}$$
$$d_x d_{zx} + d_y d_{zy} + d_z d_{zz} = 0. \tag{14}$$

In particular the two dimensional case can be derived by assuming that the distance function is constant in z.

Two dimensions. In that case the Jacobian matrix $\frac{\partial P_\Gamma}{\partial \mathbf{x}}$ of the closest point projection map is

$$\frac{\partial P_\Gamma}{\partial \mathbf{x}} = \begin{pmatrix} 1 - d_x^2 - dd_{xx} & -(d_y d_x + d d_{yx}) \\ -(d_x d_y + d d_{xy}) & 1 - d_y^2 - d d_{yy} \end{pmatrix}.$$

Since Schwartz' Theorem holds, we have $d_{xy} = d_{yx}$ making $\frac{\partial P_\Gamma}{\partial \mathbf{x}}$ a real symmetric matrix. It is therefore diagonalizable with eigenvalues 0 and $1 - d\Delta d$. Indeed, we have

$$\frac{\partial P_\Gamma}{\partial \mathbf{x}} \nabla d = \begin{pmatrix} d_x(\underbrace{1 - d_x^2 - d_y^2}_{=0 \text{ by (10) in 2D}}) - d(\underbrace{d_x d_{xx} + d_y d_{yx}}_{=0 \text{ by (12) in 2D}}) \\ \\ d_y(\underbrace{1 - d_x^2 - d_y^2}_{=0 \text{ by (10) in 2D}}) - d(\underbrace{d_y d_{yy} + d_x d_{xy}}_{=0 \text{ by (13) in 2D}}) \end{pmatrix} = \mathbf{0},$$

and for $\mathbf{v} = \begin{pmatrix} -d_y \\ d_x \end{pmatrix}$,

$$\begin{aligned} \frac{\partial P_\Gamma}{\partial \mathbf{x}} \mathbf{v} &= \begin{pmatrix} -d_y + d_y d_x^2 + d_y d d_{xx} - d_x^2 d_y - d d_x d_{xy} \\ d_y^2 d_x + d_y d d_{xx} - d_y^2 d_x - d_x d d_{yy} \end{pmatrix} \\ &= \begin{pmatrix} -d_y \\ d_x \end{pmatrix} + d \begin{pmatrix} d_y d_{xx} - d_x d_{xy} \\ d_y d_{xy} - d_x d_{yy} \end{pmatrix} \\ &= v + d \begin{pmatrix} -\Delta d(-d_y) - \underbrace{(d_y d_{yy} + d_x d_{xy})}_{=0 \text{ by (13) in 2D}} \\ \\ -\Delta d(dx) + \underbrace{d_x d_{xx} + d_y d_{xy}}_{=0 \text{ by (12) in 2D}} \end{pmatrix} \\ &= (1 - d\Delta d)\mathbf{v}. \end{aligned}$$

Since $||\mathbf{v}|| = 1$, $\mathbf{v}$ is an eigenvector corresponding to the eigenvalue $\lambda = 1 - d\Delta d$. Thus, for $\mathbf{x}$ such that $d(\mathbf{x}) = \eta$ we have that the eigenvalue λ of $\frac{\partial P_\Gamma}{\partial \mathbf{x}}$ satisfies

$$\lambda = 1 - \eta \Delta d = 1 + \eta \kappa_\eta$$

by (11). Since $1 + \eta\kappa_\eta \geq 0$, it follows that λ coincides with the singular value of $\frac{\partial P_\Gamma}{\partial \mathbf{x}}$ and hence

$$\sigma_1 = 1 + \eta \kappa_\eta.$$

Three dimensions. Since for $|\eta|$ sufficiently close to 0 the distance function is C^2, the Jacobian matrix

$$\frac{\partial P_\Gamma}{\partial \mathbf{x}} = \begin{pmatrix} 1 - d_x^2 - dd_{xx} & -(d_y d_x + d d_{yx}) & -(d_z d_x + d d_{zx}) \\ -(d_x d_y + d d_{xy}) & 1 - d_y^2 - d d_{yy} & -(d_z d_y + d d_{zy}) \\ -(d_x d_z + d d_{xz}) & -(d_y d_z + d d_{yz}) & 1 - d_z^2 - d d_{zz} \end{pmatrix},$$

is a real symmetric matrix which is diagonalizable with one zero eigenvalue and two other eigenvalues λ_1 and λ_2. Indeed using (12),(13),(14) and (10) we can show that

$$\frac{\partial P_\Gamma}{\partial \mathbf{x}} \nabla d = \mathbf{0}.$$

Now consider $\mathbf{x}$ such that $d(\mathbf{x}) = \eta$. Then, the characteristic polynomial $\chi(\lambda)$ of $\frac{\partial P_\Gamma}{\partial \mathbf{x}}$ is

$$\chi(\lambda) = -\lambda \left(\lambda^2 - (2 - \eta\Delta d)\lambda - Q \right),$$

where $Q = -G_\eta \eta^2 + \eta\Delta d - 1$ with G_η defined in (5). Since the other two eigenvalues of $\frac{\partial P_\Gamma}{\partial \mathbf{x}}$ are the solutions of the quadratic equation $\lambda^2 - (2 - \eta\Delta d)\lambda - Q = 0$, it follows that

$$\lambda_1 \lambda_2 = -Q = 1 - \eta\Delta d + \eta^2 G_\eta = 1 + 2\eta H_\eta + \eta^2 G_\eta.$$

Since $1 + 2\eta H_\eta + \eta^2 G_\eta \geq 0$, it follows that

$$\sigma_1 \sigma_2 = 1 + 2\eta H_\eta + \eta^2 G_\eta,$$

where σ_1 and σ_2 are singular values of $\frac{\partial P_\Gamma}{\partial \mathbf{x}}$. □

This leads to the following proposition:

Theorem 3. *Consider Γ a curve in 2D or surface in 3D with C^2 boundaries if it is not closed, and define $d : \mathbb{R}^n \mapsto \mathbb{R}^+ \cup \{0\}$ $(n = 2, 3)$ to be the distance function to Γ with $P_\Gamma : \mathbb{R}^n \mapsto \Gamma$ the closest point mapping to Γ. Then*

$$\int_\Gamma v(\mathbf{x}) d\mathbf{x} = \int_{\mathbb{R}^n} v(P_\Gamma(\mathbf{x}) \delta_\epsilon(d(\mathbf{x})) \Sigma(\mathbf{x}) d\mathbf{x}, \tag{15}$$

where δ_ϵ is an averaging kernel and $\Sigma(\mathbf{x})$is defined as

$$\Sigma(\mathbf{x}) = \begin{cases} \sigma_1(\mathbf{x}), & n = 2, \\ \sigma_1(\mathbf{x})\sigma_2(\mathbf{x}), & n = 3, \end{cases}$$

where $\sigma_j(\mathbf{x})$, $j = 1, 2$, is the j-th singular value of the Jacobian matrix, $\frac{\partial P_\Gamma}{\partial \mathbf{x}}$ evaluated at $\mathbf{x}$.

Proof. If Γ is closed we combine Equation (2) with the result $J(\mathbf{x}) = \Sigma(\mathbf{x})$ from Equation (9) of Proposition 2.

If Γ is open there is a little more to show since Equation (2) was only derived for closed manifolds. Before we state the result, it is necessary to understand how Γ_η defined in (8) (an $\eta-$level set of d) looks like for an open curve in two dimensions and for a surface with boundaries in three dimensions.
In two dimensions, Γ_η consists of a flat tubular part on either side of the curve and two semi circles at the two ends of the curve. See Figure 1.
In three dimensions Γ is in general made up of three distinct parts: the interior part, the edges of the boundary and the corners. If we assume that Γ has N edges then

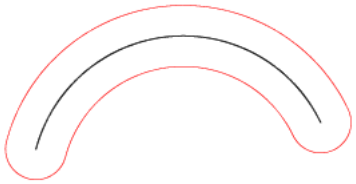

Figure 1: An example of an open curve Γ (black curve) and its η-level set Γ_η (red curve). Γ_η consists of a tubular part and two semi circles at the two ends.

we can write $\Gamma = \Gamma^o \cup (\cup_{i=1}^N E_i) \cup (\cup_{i=1}^N C_i)$, where Γ^o is the interior of Γ, E_i is the i-th edge of the boundary of Γ and C_i is its i -th corner. In that setting we can write $\Gamma_\eta = I_\eta \cup (\cup_{i=1}^N T_i^\eta) \cup (\cup_{i=1}^N S_i^\eta)$, where I_η is the inside portion of Γ_η, T_i^η is the cylindrical part of Γ_η representing the set of points located at a distance η from the i -th edge E_i, and finally S_i^η is the spherical part of Γ_η representing the set of points located at a distance η from the i -th corner C_i. See Figure 2.

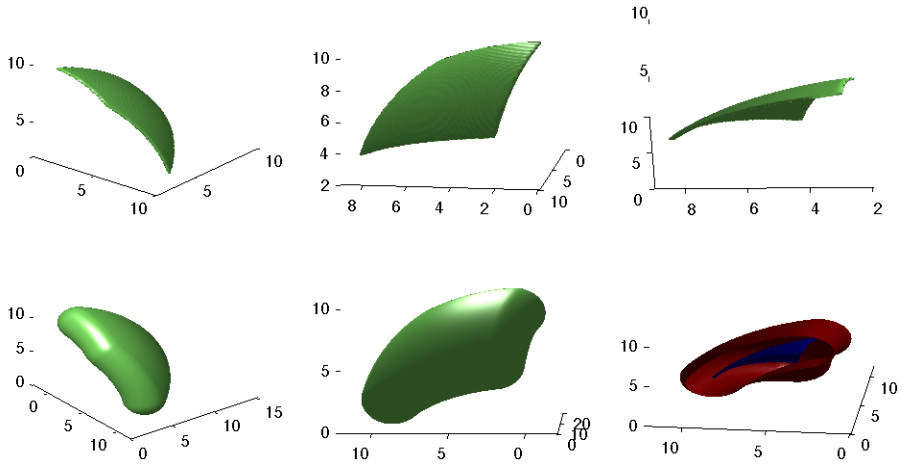

Figure 2: An example of a surface with boundaries viewed from different angles (2(a), 2(b) and 2(c)) and its corresponding η-level set Γ_η viewed from the same angles (2(d), 2(e) and 2(f)). Figure 2(f) shows the surface and Γ_η.

In both cases we need to integrate over Γ_η and then subtract the two semi circles at the two end points of the curve (in two dimensions) or subtract the portions of sphere at the corners of the surface and the portions of cylinders at the edges of the surface (in three dimensions). However, it turns out that the subtraction is unnecessary since $\Sigma(\mathbf{x}) = 0$ on each of the subtracted pieces as shown below.

- **Two dimensions.** On the semi-circle around the end point of a curve, the closest point mapping is *constant* since all points on the semi-circle Γ_η map to the end point. As a result, the singular values of the Jacobian matrix of the closest point mapping are all zeros and thus $\Sigma(\mathbf{x}) = 0$ on the semi-circles around the end points of a curve.

- **Three dimensions.** As in two dimensions, on the portions of sphere around a corner point of a surface, the closest point mapping is *constant* and thus $\Sigma(\mathbf{x}) = 0$. On the portion of cylinders, the closest point mapping is constant along the radial dimension (one of the principal directions or singular vector) resulting of the singular value along that direction to be zero. Since $\Sigma(\mathbf{x})$ is the product of the singular values, it follows that $\Sigma(\mathbf{x}) = 0$ on the portion of cylinders as well.

Consequently, Equation (15) holds for any C^2 curve or surface with C^2 boundaries of codimension 1. □

2.2 Codimension 2

We consider a C^2 curve in $\mathbb{R}^3$ denoted by Γ and let $\gamma(s)$ be a parameterization by arclength of Γ. We denote by $d : \mathbb{R}^3 \mapsto \mathbb{R}^+ \cup \{0\}$ the distance function to Γ and let $P_\Gamma : \mathbb{R}^3 \mapsto \Gamma$ be the closest point mapping to Γ. We consider a parameterization of the *tubular part* of the level surface for $\eta \in [0, \epsilon]$ defined as

$$\mathbf{x}(s, \theta, \eta) : \gamma(s) + \eta \cos\theta \vec{\mathbf{N}}(s) + \eta \sin\theta \vec{\mathbf{B}}(s),$$

where $\vec{\mathbf{T}} = \frac{d\gamma}{ds}$, $\vec{\mathbf{N}}$ and $\vec{\mathbf{B}}$ constitute the Frenet frame for γ as illustrated in Figure 3. As in the previous section, if Γ is closed then d is the signed distance function to Γ .

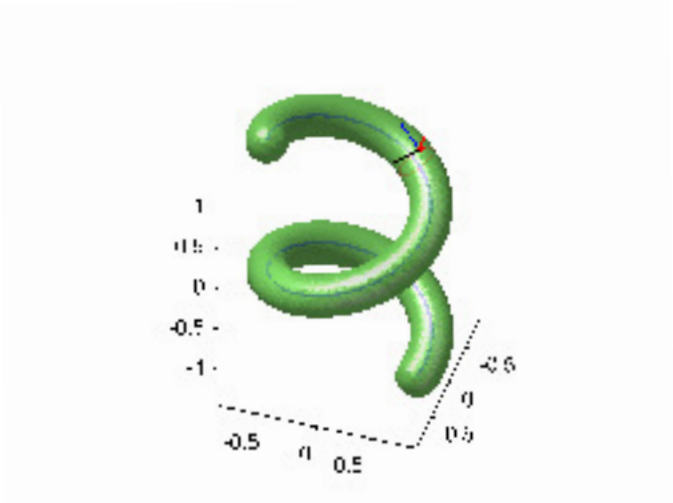

Figure 3: Three dimensional curve with its η-level surface Γ_η in green and the Frenet frame at a point on Γ_η.

If we project a point $\mathbf{x}$ on the tubular part of the level surface Γ_η defined in (8),

we have $P_\Gamma(\mathbf{x}(\mathbf{s},\theta,\eta)) = \gamma(\mathbf{s})$. If L is the length of the curve it follows that

$$\begin{aligned}\int_0^{2\pi}\int_0^L g(P_\Gamma(\mathbf{x}(\mathbf{s},\theta,\eta)))|\mathbf{x_s}\times\mathbf{x}_\theta|dsd\theta &= \int_0^{2\pi}\int_0^L g(\gamma(s))\eta(1-\eta\kappa(s)\cos\theta)dsd\theta, \\ &= \eta\int_0^L g(\gamma(s))\int_0^{2\pi}(1-\eta\kappa\cos\theta)d\theta ds, \\ &= 2\pi\eta\int g(\gamma(s))ds.\end{aligned} \tag{16}$$

Note that the tubular part of the level surface Γ_η does not contain the two hemispheres of Γ_η which are located at the two end points of the curve Γ. Thus,

$$\int_{\Gamma_\eta\setminus\{C_1\cup C_2\}} g(P_\Gamma(\mathbf{x}))dS_\mathbf{x} = 2\pi\eta\int_\Gamma g ds, \tag{17}$$

where C_1 and C_2 are the two hemispheres of the level surface Γ_η located at the two end points of the curve Γ. Consequently, for sufficiently small ϵ and by the coarea formula we obtain

$$\begin{aligned}\int_\Gamma g(\gamma(s))ds &= \frac{1}{2\pi}\int_0^\epsilon\left(\frac{1}{\eta}\int_{\Gamma_\eta\setminus\{C_1\cup C_2\}} g(P_\Gamma(\mathbf{x}))\right)K_\epsilon(\eta)d\eta, \\ &= \frac{1}{2\pi}\int_{\mathbb{R}^3} g(P_\Gamma(\mathbf{x}))\frac{K_\epsilon(d)}{d}\chi_{(C_1\cup C_2)^c}(\mathbf{x})d\mathbf{x},\end{aligned}$$

where K_ϵ is a C^1 averaging kernel supported in $[0,\epsilon]$ and $\chi_{(C_1\cup C_2)^c}(\mathbf{x})$ is the characteristic function of the set $(C_1\cup C_2)^c$. In our numerical simulations we consider the kernel

$$K_\epsilon^{1,1}(\eta) = \frac{1}{\epsilon}\left(1-\cos\left(2\pi\frac{\eta}{\epsilon}\right)\right)\chi_{[0,\epsilon]}(\eta). \tag{18}$$

Since the formulation above does not use the two hemispheres located at both end points of the curve, in order to integrate over the tubular part of Γ_η only, it is necessary to subtract the integration over each of the hemispheres C_1 and C_2 . The result can be summarized in the following proposition:

Proposition 4. *Consider a single C^2 curve Γ in $\mathbb{R}^3$ parameterized by $\gamma(s)$ where s is the arclength parameter, and let d be the distance function to Γ. We define K_ϵ to be a C^1 averaging kernel compactly supported in $[0,\epsilon]$ and $P_\Gamma : \mathbb{R}^3 \mapsto \Gamma$ to be the closest point mapping to Γ.*

If g is a continuous function defined on Γ then for sufficiently small $\epsilon > 0$ we have

$$\int_\Gamma g(\gamma(s))ds = \frac{1}{2\pi}\int_{\mathbb{R}^3} g(P_\Gamma(\mathbf{x}))\frac{K_\epsilon(d(\mathbf{x}))}{d(\mathbf{x})}d\mathbf{x} - 2\int_0^\epsilon g(\mathbf{x}_\eta)\eta K_\epsilon(\eta)d\eta, \tag{19}$$

where $\mathbf{x}_\eta$ is a point on a sphere of radius η.

Note that for the computation of the length of a curve, the correction terms given by integrating over both C_1 and C_2 is

$$\int_0^\epsilon \frac{K_\epsilon(\eta)}{\eta}|\mathbb{S}^1|d\eta = \int_0^\epsilon \frac{K_\epsilon(\eta)}{\eta}4\pi\eta^2 d\eta = 2\pi\epsilon.$$

This simple correction is, however, not suitable for more general cases that contain multiple curve segments and several integrands. We shall derive a more elegant and seamless way to perform such correction in the following section.

Now if we consider a C^2 curve in three dimensions and let P_Γ be its closest point mapping, we have the following proposition:

Theorem 5. *Let $\sigma(\mathbf{x})$ be the nonzero singular value of $\frac{\partial P_\Gamma}{\partial \mathbf{x}}$ and let g be a continuous function defined on Γ. If $\gamma(s)$ is the arclength parameterization of Γ and if ϵ is sufficiently small we have*

$$\int_\Gamma g(\gamma(s))ds = \frac{1}{2\pi}\int_{\mathbb{R}^3} g(P_\Gamma(\mathbf{x}))\frac{K_\epsilon(d)}{d}\sigma(\mathbf{x})d\mathbf{x}, \tag{20}$$

where d is the distance function to Γ.

Proof. Let $\mathbf{x} \in \mathbb{R}^3$. Then there exists $\eta > 0$, such that $\mathbf{x} \in \Gamma_\eta$.

Case 1: $\mathbf{x}$ is on the *spherical part* of Γ_η corresponding to the η-distance to either of the two end points of the curve Γ. WLOG we assume that $\mathbf{x}$ is at a distance η from the first end point C_1 parameterized by $\gamma(0)$. The result is the same if $\mathbf{x}$ is on the other sphere, i.e. at a distance η from the other end point C_2. In that case, $P_\Gamma(\mathbf{x}) = \gamma(0)$ for all $\mathbf{x}$ on the spherical part so that the Jacobian matrix $\frac{\partial P_\Gamma(\mathbf{x})}{\partial \mathbf{x}} = 0$. Therefore, for $\mathbf{x}$ on the spherical part of Γ_η, all singular values of the Jacobian matrix are zero.

Case 2: $\mathbf{x}$ is on the *tubular part* of Γ_η. In that case, if we use the Frenet frame centered at the point $\mathbf{x} = \mathbf{x}(s, \theta, \eta) \in \Gamma_\eta$, we can write $\mathbf{x}$ in the new coordinate system $(\vec{\mathbf{T}}, \vec{\mathbf{N}}, \vec{\mathbf{B}})$ as

$$\mathbf{x} = \gamma(s) + v\vec{\mathbf{N}} + w\vec{\mathbf{B}}, \tag{21}$$

where $u = 0$ is the coordinate of $\mathbf{x}$ along $\vec{\mathbf{T}}$, v is the coordinate along $\vec{\mathbf{N}}$ and w is the coordinate along $\vec{\mathbf{B}}$. Since the projection $P_\Gamma(\mathbf{x}) = \gamma(s)$ does not depend on v nor w (since the plane $(\vec{\mathbf{N}}, \vec{\mathbf{B}})$ is normal to the curve Γ) is follows that

$$\frac{\partial P_\Gamma(\mathbf{x})}{\partial v} = \frac{\partial P_\Gamma(\mathbf{x})}{\partial w} = 0.$$

On the other hand, we have

$$\frac{\partial P_\Gamma(\mathbf{x})}{\partial u} = \frac{\partial \gamma(s)}{\partial u} = \frac{\partial s}{\partial u}\frac{\partial \gamma(s)}{\partial s} = \frac{\partial s}{\partial u}\vec{\mathbf{T}},$$

where $\frac{\partial s}{\partial u}$ is the variation of the arclength parameter s with respect to u when the point $\mathbf{x}$ is moving on Γ_η along the tangential direction $\vec{\mathbf{T}}$. Since u is the arclength parameter along the tangential direction $\vec{\mathbf{T}}$, it follows that we have a unit speed parameterization along $\vec{\mathbf{T}}$ giving the identity

$$\frac{\partial \mathbf{x}}{\partial u} \cdot \vec{\mathbf{T}} = 1.$$

In addition,

$$\begin{aligned}\frac{\partial \mathbf{x}}{\partial s} &= \frac{\partial \gamma(s)}{\partial s} + v\frac{\vec{\mathbf{N}}}{\partial s} + w\frac{\vec{\mathbf{B}}}{\partial s} \\ &= \vec{\mathbf{T}} - \kappa v\vec{\mathbf{T}} + \tau v\vec{\mathbf{B}} - \tau w\vec{\mathbf{N}} \\ &= (1-\kappa v)\,\vec{\mathbf{T}} - \tau w\vec{\mathbf{N}} + \tau v\vec{\mathbf{B}},\end{aligned}$$

where κ is the curvature of Γ at $\gamma(s)$ and τ is the torsion of the curve Γ at the point $\gamma(s)$. Since the level surface Γ_η is a tube of radius η, its intersection with the normal plane $(\vec{\mathbf{N}}, \vec{\mathbf{B}})$ is a circle of radius η. Hence if we use polar coordinates on the normal plane, we obtain $v = \eta\cos\theta$ and $w = \eta\sin\theta$. It follows that

$$\frac{\partial \mathbf{x}}{\partial s} \cdot \vec{\mathbf{T}} = 1 - \kappa\eta\cos\theta.$$

Consequently we have

$$\frac{\partial \mathbf{x}}{\partial u} \cdot \vec{\mathbf{T}} = 1 = \frac{\partial s}{\partial u}\frac{\partial \mathbf{x}}{\partial s} \cdot \vec{\mathbf{T}} = \frac{\partial s}{\partial u}(1 - \kappa\eta\cos\theta),$$

and

$$\frac{\partial s}{\partial u} = \frac{1}{1-\kappa\eta\cos\theta}.$$

Therefore, in the Frenet frame, the Jacobian matrix of the closest point projection map can be written as

$$\frac{\partial P_\Gamma}{\partial \mathbf{x}} = \begin{pmatrix} \frac{1}{1-\kappa\eta\cos\theta} & 0 & 0 \\ 0 & 0 & 0 \\ 0 & 0 & 0 \end{pmatrix},$$

where $\frac{1}{1-\kappa\eta\cos\theta}$ is the nonzero eigenvalue of the Jacobian of the closest point mapping. Since $\frac{1}{1-\kappa\eta\cos\theta} \geq 0$, it is also its singular value $\sigma(\mathbf{x})$.

Therefore we have

$$\sigma(\mathbf{x}) = \begin{cases} 0 & \text{if } \mathbf{x} \text{ is on the spherical part of } \Gamma_\eta, \\ \frac{1}{1-\kappa\eta\cos\theta} & \text{if } \mathbf{x} \text{ is on the tubular part of } \Gamma_\eta. \end{cases} \tag{22}$$

Now using (16) and (17) we obtain

$$\begin{aligned}\int_{\Gamma_\eta} g(P_\Gamma(\mathbf{x}))\sigma(\mathbf{x})dS_{\mathbf{x}} &= \int_{\Gamma_\eta\setminus\{C_1\bigcup C_2\}} g(P_\Gamma(\mathbf{x}))\sigma(\mathbf{x})dS_{\mathbf{x}} \\ &= \int_0^{2\pi}\int_0^L g(P_\Gamma(\mathbf{x}))\sigma(\mathbf{x})|\mathbf{x_s}\times\mathbf{x}_\theta|dsd\theta \\ &= \int_0^{2\pi}\int_0^L g(\gamma(s))\eta\frac{1-\eta\kappa(s)\cos\theta}{1-\eta\kappa(s)\cos\theta}dsd\theta \\ &= 2\pi\eta\int_0^L g(\gamma(s))ds\end{aligned}$$

It follows that for K_ϵ a C^1 averaging kernel compactly supported in $[0,\epsilon]$, for sufficiently small ϵ and by the coarea formula, we have

$$\begin{aligned}\int_\Gamma g ds &= \frac{1}{2\pi}\int_0^\epsilon \frac{1}{\eta}\int_{\Gamma_\eta} g(P_\Gamma(\mathbf{x}))\sigma(\mathbf{x})K_\epsilon(\eta)d\eta \\ &= \frac{1}{2\pi}\int_{\mathbb{R}^3} g(P_\Gamma(\mathbf{x}))\frac{K_\epsilon(d)}{d}\sigma(\mathbf{x})d\mathbf{x}.\end{aligned}$$

□

3 Numerical simulations

In this section we investigate the convergence of our numerical integration using simple Riemann sum over uniform Cartesian grids. In our computations we use the cosine kernel

$$K_\epsilon^{\cos}(\eta) = \chi_{[0,\epsilon]}(\eta)\frac{1}{2\epsilon}\left(1+\cos\left(\frac{\pi\eta}{\epsilon}\right)\right)$$

for integration on surfaces of codimension 1, and the kernel $K_\epsilon^{1,1}$ defined in (18) for codimension 2. Unless stated otherwise, the singular values are computed from the matrix whose elements are computed by the standard central difference approximations of the Jacobian matrix $\frac{\partial P_\Gamma}{\partial \mathbf{x}}$. With these compactly supported kernels, formulas (15) and (20) can be considered integration of functions defined on suitable hypercubes, periodically extended. In such settings, simple Riemann sums on Cartesian grids are equivalent to sums suing Trapezoidal rule, and the order of accuracy will be related in general to the smoothness of the integrands; exception can be found when the normals of the surfaces are rationally dependent on the step sizes used in the Cartesian grids.

3.1 Integration of codimension one surfaces

We tested our numerical integration on two different portions of circle, a torus, a quarter sphere and a three quarter sphere. We computed their respective lengths or

surface areas by integrating the constant 1 over the curve or surface. Each of these tests were designed to exhibit the convergence rate of our formulations on cases with varying difficulty. In particular, the convergence rate of our formulation depends on the smoothness of the closest point mapping inside the tubular neighborhood of the surfaces.

The results for the portions of circle are given in Tables 1 and 2. In the first convergence studies (Table 1) the line where the closest point mapping has a jump discontinuity is parallel to the grid lines. In this case we see a second order convergence rate using central differencing to compute the Jacobian matrix $\frac{\partial P_\Gamma}{\partial \mathbf{x}}$. In the second test case however, the portion of circle is chosen so that the line where the closest point mapping has a jump discontinuity is not parallel to the grid lines. In that case the normal to the curve is rationally dependent on the step size of the Cartesian grid and the convergence rate reduces to first order even though we used central differencing to compute $\frac{\partial P_\Gamma}{\partial \mathbf{x}}$. We note that in these two tests, we chose ϵ (the half width of the tubular neighborhood around the curve) small enough so that the line where the closest point mapping is discontinuous is outside of it.

In three dimensions we first tested our method on a torus (closed smooth surface). The results for the torus are reported in Table 3. In this case the closest point mapping is very smooth and we see third order convergence when using a third order difference scheme to approximate $\frac{\partial P_\Gamma}{\partial \mathbf{x}}$. For surfaces with boundaries we tested the method on a quarter sphere and a three quarter sphere. The three quarter sphere case is illustrated in Figure 4.

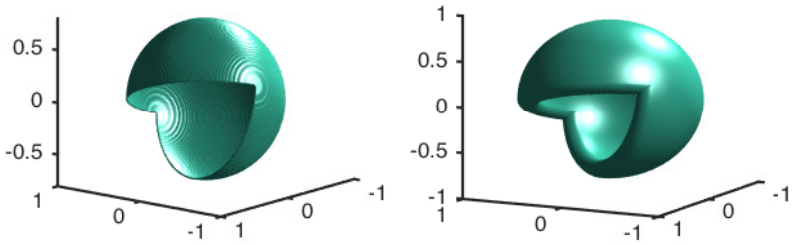

Figure 4: The three quarter sphere (4(a)) and its corresponding η-level set Γ_η (4(b)).

The reason for choosing these two cases is because the closest point mapping has a different degree of smoothness for each of these surfaces. For the quarter sphere the closest point mapping is smooth enough, but for the three quarter sphere, the tubular neighborhood around the surface contains the line where the closest point mapping has a jump discontinuity. In that latter case, it is therefore necessary to use an adequate one sided discretization to compute $\frac{\partial P_\Gamma}{\partial \mathbf{x}}$ accurately. The one-sided discretization that we used is reported in Section 3.3. The test for the quarter sphere still uses central differencing to compute $\frac{\partial P_\Gamma}{\partial \mathbf{x}}$. The results for the portions of sphere are reported in Tables 4 and 5.

Table 1: Relative errors in the numerical approximation of the length of a planar curve, which is a portion of circle of radius $R = 0.75$ centered at 0. The width for the tubular neighborhood of the curve is $\epsilon = 0.2$. In this computation, the closest point mapping has a jump discontinuity along a straight-line which is arranged to be parallel to the grid lines.

n	Relative Error	Order
64	2.7994×10^{-4}	–
128	7.0665×10^{-5}	1.99
256	1.7187×10^{-5}	2.04
512	4.2719×10^{-6}	2.01
1024	1.0636×10^{-6}	2.01
2048	2.6567×10^{-7}	2.00
4096	6.6045×10^{-8}	2.01
8192	1.6513×10^{-8}	2.00

Table 2: Relative errors in the numerical approximation of the length of a planar curve, which is a portion of circle of radius $R = 0.75$ centered at 0. The width for the tubular neighborhood of the curve is $\epsilon = 0.2$. In this computation, the jump discontinuity of the closest point mapping is not parallel to the grid lines.

n	Relative Error	Order
64	3.7159×10^{-5}	–
128	2.5786×10^{-7}	7.17
256	4.2361×10^{-6}	-4.04
512	3.2246×10^{-6}	0.39
1024	1.8876×10^{-6}	0.77
2048	1.0132×10^{-7}	0.90
4096	5.2372×10^{-7}	0.95
8192	2.6615×10^{-7}	0.98

Table 3: Relative errors in the numerical approximation of the surface area of a torus centered at 0. The distance from the center to the tube that form the torus is $R = 0.75$ and the radius of the tube is $r = 0.25$. In this computation, we summed up grid points that are within $\epsilon = 0.2$ distance from the surface. The Jacobian matrix $\frac{\partial P_\Gamma}{\partial \mathbf{x}}$ is approximated by a standard third order accurate differencing.

n	Relative Error	Order
32	6.2030×10^{-3}	–
64	1.8073×10^{-4}	5.10
128	6.6838×10^{-6}	4.76
256	4.1530×10^{-7}	4.01
512	5.0379×10^{-8}	3.04

Table 4: Relative errors in the numerical approximation of the surface area of a quarter sphere with radius $R = 0.75$ centered at 0. In this computation, we summed up grid points that are within $\epsilon = 0.2$ distance from the surface. We used the standard central difference scheme to compute each entry of the Jacobian matrix $\frac{\partial P_\Gamma}{\partial \mathbf{x}}$.

n	Relative Error	Order
32	9.2825×10^{-3}	–
64	1.8365×10^{-3}	2.34
128	2.7726×10^{-4}	2.73
256	7.1886×10^{-5}	1.95
512	1.4811×10^{-5}	2.30

Table 5: Relative errors in the numerical approximation of the surface area of a 3/4 sphere with radius $R = 0.75$ centered at 0 (this is the portion of a sphere that misses half of a hemisphere). In this computation, we summed up grid points that are within $\epsilon = 0.2$ distance from the surface. Due to this setup, the closest point mapping has a discontinuity that stems out from the boundary of the surface. We used the discretization described in Section 3.3 to compute each entry of the Jacobian matrix $\frac{\partial P_\Gamma}{\partial \mathbf{x}}$.

n	Relative Error	Order
32	1.1726×10^{-2}	–
64	1.1733×10^{-3}	3.32
128	9.1325×10^{-4}	0.36
256	3.8238×10^{-4}	1.26
512	7.8308×10^{-5}	2.29

3.2 Integrating along curves in three dimensions

In codimension 2, we tested our numerical integration on a coil wrapped around the helix defined parametrically as

$$\mathbf{x}(t) = (r\cos(t), r\sin(t), bt)\,,$$

with $r = 0.75$ and $b = 0.25$. The coil is then wrapped around the helix at a distance of 0.2 from the helix. As our test case, we computed the length of the coil by integrating 1 along the curve. The results are reported in Table 6.

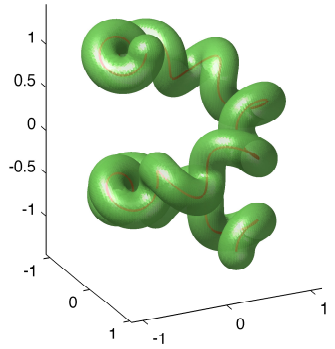

Figure 5: The coil and one of the level sets of the distance function to the coil used in the reported numerical simulations.

Table 6: Relative errors in the numerical approximation of a coil wrapped around a helix. In this computation, we used a constant width for the tubular neighborhood $\epsilon = 0.1$ and took the averaging kernels to be $K_\epsilon^{1,1}$ defined in (18).

n	Relative Error	Order
60	5.5078×10^{-3}	–
120	1.1476×10^{-3}	2.63
240	2.3409×10^{-4}	2.29
480	3.7166×10^{-5}	2.66

3.3 One-sided discretization of the Jacobian matrix

Here for completeness, we describe the one-sided discretization used in computing results reported in Table 5.

For simplicity, we will describe the one-sided discretization for a uniform Cartesian grid, namely for $P_\Gamma(\mathbf{x}_{i,j}) = (U_{i,j}, V_{i,j})$ with $\mathbf{x}_{i,j} = (ih, jh)$, $i, j \in \mathbb{Z}$ and $h > 0$ being

the step size. The Jacobian matrix will be approximated by simple finite differences defined below:

$$\frac{\partial P_\Gamma}{\partial \mathbf{x}}(\mathbf{x}_{i,j}) \approx \begin{pmatrix} (U_x)_{i,j} & (U_y)_{i,j} \\ (V_x)_{i,j} & (V_y)_{i,j} \end{pmatrix}.$$

The discretization of U and V have to be defined together because the two functions are not independent of each other. With

$$(U_x^{\pm})_{i,j} := \pm\frac{1}{2h}\left(-3U_{i,j} + 4U_{i\pm1,j} - U_{i\pm2,j}\right),$$

and the smoothness indicator

$$S_{i,j}^{\pm} = S^{\pm}(U_{i,j}) := \triangle^{+}\triangle^{-}U_{i\pm1,j}$$

we define

$$(U_x)_{i,j} := \begin{cases} (U_x^{+})_{i,j}, & \text{if } |S_{i,j}^{+}| \le |S_{i,j}^{-}|, \\ (U_x^{-})_{i,j}, & \text{otherwise,} \end{cases}$$

and $(V_x)_{i,j}$ is defined according to the choice of stencil based on $S^{\pm}(U_{i,j})$

$$(V_x)_{i,j} := \begin{cases} (V_x^{+})_{i,j}, & \text{if } |S_{i,j}^{+}| \le |S_{i,j}^{-}|, \\ (V_x^{-})_{i,j}, & \text{otherwise.} \end{cases}$$

The discretization of U_y and V_y is defined similarly with the choice of the stencil based on $S^{\pm}(V_{i,j})$.

4 Summary

In this paper, we presented a new approach for computing integrals along curves and surfaces that are defined either implicitly by the distance function to these manifolds or by the closest point mappings. We are motivated by the abundance of discrete point sets sampled from surfaces using devices such as LIDAR, the need to compute functionals defined over the underlying surfaces, as well as many applications involving the level set method or the use of closest point methods.

Contrary to most other existing approximations using either smeared out Dirac delta functions or locally obtained parameterized patches, we derive a volume integral in the embedding Euclidean space which is equivalent to the desired surface or line integrals. This allows for easy construction of higher order numerical approximations of these integrals. The key components of this new approach include the use of singular values of the Jacobian matrix of the closest point mapping, which can be computed easily to high order even by simple finite differences.

Acknowledgement

The second author thanks Prof. Steve Ruuth for stimulating conversations. Kublik's research was partially funded by a University of Dayton Research Council Seed Grant and Tsai's research is partially supported by Simons Foundation, NSF Grants DMS-1318975, DMS-1217203, and ARO Grant No. W911NF-12-1-0519.

References

[1] M. C. Delfour and J.-P. Zolesio. Shapes and geometries. matrices, analysis, differential calculus, and optimization. *Advances in Design and Control, SIAM*, 2001.

[2] J. Dolbow and I. Harari. An efficient finite element method for embedded interface problems. *J. Numer. Methods Eng.*, 78:229–252, 2009.

[3] B. Engquist, A.-K. Tornberg, and R. Tsai. Discretization of dirac delta functions in level set methods. *J. Comput. Phys.*, 207(1):28–51, 2005.

[4] H. Federer. Curvature measures. *Transactions of the American Mathematical Society*, 93:418–491, 1959.

[5] H. Federer. *Geometric Measure Theory*. Springer-Verlag, 1969.

[6] N. J. Hicks. Notes on differential geometry, 1965.

[7] C. Kublik, N. M. Tanushev, and R. Tsai. An Implicit Interface Boundary Integral Method for Poisson's Equation on Arbitrary Domains. *J. Comput. Phys.*, 247:269–311, 2013.

[8] C. B. Macdonald, J. Brandman, and S. J. Ruuth. Solving eigenvalue problems on curved surfaces using the Closest Point Method. *J. Comput. Phys.*, 230(22):7944–7956, 2011.

[9] C. B. Macdonald and S. J. Ruuth. Level set equations on surfaces via the Closest Point Method. *J. Sci. Phys.*, 35(2-3):219–240, 2008.

[10] C. B. Macdonald and S. J. Ruuth. The implicit Closest Point Method for the numerical solution of partial differential equations on surfaces. *SIAM J. Sci. Comput.*, 31(6):4330–4350, 2009.

[11] S. Osher and R.Fedkiw. *Level Set Methods and Ddynamics Implicit Surfaces*. Springer-Verlag, 2002.

[12] S. Osher and J. A. Sethian. Fronts propagating with curvature dependent speed: Algorithms based on hamilton-jacobi formulations. *J. Comp. Phys.*, 79:12–49, 1988.

[13] S. J. Ruuth and B. Merriman. A simple embedding method for solving partial differential equations on surfaces. *J. Comput. Phys.*, 227(3):1943–1961, 2008.

[14] J. A. Sethian. *Level Set Methods and Fast Marching Methods*. Cambridge University Press, 1999.

[15] P. Smereka. The numerical approximation of a delta function with application to level set methods. *J. Comput. Phys.*, 211(1):77–90, 2006.

[16] J. D. Towers. Two methods for discretizing a delta function supported on a level set. *J. Comput. Phys.*, 220(2):915–931, 2007.

[17] S. Zahedi and A.-K. Tornberg. Delta function approximations in level set methods by distance function extension. *J. Comput. Phys.*, 229(6):2199–2219, 2010.